1972MNRAS.160....1W

Mon. Not. R. astr. Soc. (1972) **160**, 1–14.

INFRA-RED SOURCES IN THE H II REGION W3

C. G. Wynn-Williams, E. E. Becklin and G. Neugebauer

(Received 1972 July 24)

SUMMARY

High resolution mapping and photometric observations in the wavelength range 1·65–20 μ have led to the discovery of nine distinct infra-red objects in W3. Four of them, including one coincident with W3(OH), are identified with compact radio H II condensations $\sim$0·1 pc in diameter. They show strong emission in the range 3–20 μ which is attributable to dust grains at a temperature of $\sim$150 K mixed with the ionized gas. On the other hand, the 2-μ emission from these objects is considerably less than is predicted from the radio measurements, indicating that the H II condensations are surrounded by obscuring dust with up to 50 mag of visual extinction. One of the condensations contains an unresolved source which is almost certainly a highly obscured O star that excites the component. Four other infra-red sources have no associated radio continuum source; one of these, an unresolved source with a luminosity $\sim 3 \times 10^4\ L_\odot$, is coincident with a source of H_2O maser emission and may be a massive protostar.

1. INTRODUCTION

W3, a powerful galactic radio source, is an H II region situated in the Perseus spiral arm at a distance of about 3 kpc.* It is associated with the optical nebula IC 1795, at least two centres of molecular maser emission and large quantities of dust and neutral hydrogen.

Recent aperture synthesis maps of W3 at 2·7 GHz and 5 GHz (Webster & Altenhoff 1970; Wynn-Williams 1971) show that a large fraction of the total radio emission originates from compact condensations with diameters of the order of 0·1 pc and electron densities of about 10^4 cm^{-3}. A reproduction of the Sky Survey red photograph of the region is included in the paper by Wynn-Williams (1971), hereafter referred to as 'Paper I'.

In this paper, we examine the infra-red emission in the range 1·65 to 20 μ from two regions of W3. These regions correspond approximately to those mapped at 5 GHz in Paper I and comprise:

1. The W3 (continuum) source. This is a 3 arc min (2·7 pc) diameter region containing four condensations, and is the main source of continuum radio emission. This region is associated with a powerful H_2O maser source and lies behind a thick layer of obscuring dust.

2. The W3(OH) source. This is a very compact H II condensation, only some 2 arc sec (0·03 pc) in diameter. It is situated about 16 arc min (14 pc) from W3 (continuum) and is associated with the main source of OH emission in W3, but no optical feature.

* The kinematic distance to W3 is 3·1 kpc (Reifenstein *et al.* 1970), while the distance to the nearby Cas OB6 association is 2·4 kpc (Becker 1963).

© Royal Astronomical Society • Provided by the NASA Astrophysics Data System

Downloaded from https://academic.oup.com/mnras/article-abstract/160/1/1/2604637 by California Institute of Technology user on 19 May 2020

1972MNRAS.160....1W

The main purposes of the present observations were (a) to search for the exciting stars of the H II condensations, which are obscured at optical wavelengths; (b) to examine the distribution of heated dust in the nebula; and (c) to see if there exist correlations between OH/H_2O and infra-red emission in H II regions similar to those that exist for OH/IR stars (see, for example, Wilson *et al.* 1972).

W3 is a particularly suitable object for study in the infra-red because (a) it has a high emission measure; (b) star formation is likely to have been taking place within the last 10^4 yr (Paper I); and (c) there already exists a large body of optical and radio data on the source.

2. OBSERVATIONS

The observations presented here consist of wide band photometric and mapping measurements at 1·65 μ (1·5–1·8 μ), 2·2 μ (2·0–2·4 μ), 3·5 μ (3·2–3·8 μ), 4·8 μ (4·5–5·1 μ), 10 μ (8–13 μ) and 20 μ (17–24 μ). Measurements were made during the winter of 1971–72 on the Hooker 100-inch and the Hale 200-inch telescopes of the Hale Observatories. The photometer used measures the difference between the emission from two adjacent areas of sky (Becklin & Neugebauer 1968). The separation of these areas depended on the choice of telescope and operating wavelength, but was usually in the range of 7–30 arc sec. Focal plane diaphragms with a variety of sizes were used, the choice depending on the seeing conditions and the nature of the object being studied. For much of the mapping and for a large number of the photometric determinations a 10 arc sec aperture was used.

Calibrations were made using standard stars. The flux calibration was based on the model atmosphere calculations of α Lyr given by Schild, Peterson & Oke (1971); the flux levels at the effective wavelengths are given in Wilson *et al.* (1972). At 20 μ the air mass correction was determined each night using a bright star at different zenith angles; standard air mass corrections were applied to the 1·65- to 10-μ data.

None of the infra-red sources under study are visible optically; their positions were therefore established relative to nearby field stars by measurements at the focal plane of the telescope. The positions of the field stars were then determined relative to a number of AGK2 stars by measurements of the appropriate 48-inch Schmidt Sky Survey plate.

3. RESULTS

Fig. 1 shows the maps of the W3 (continuum) source at 2·2 and 20 μ, together with the 6-cm radio map of the corresponding area adapted from Paper I. The whole area of Fig. 1 was surveyed down to flux density limits of 150 f.u. at 20 μ and 0·1 f.u. at 2·2 μ. Selected parts of the region were, however, studied in greater detail, with the result that sources with flux densities below the limits quoted above are included in Fig. 1. Because of the confusion with field stars, 2·2-μ sources to the west of $02^h\ 21^m\ 48^s$ are not shown.

The seven sources of infra-red emission which are evident in Fig. 1 are discussed in more detail in Sections 3(a)–3(c). Two additional infra-red sources were discovered associated with W3(OH); these are discussed in Section 3(d). Throughout this paper the numbers IRS1, IRS2, etc. refer to infra-red sources, while the numbers W3(A), W3(B), etc. refer to the radio components as in Paper I; the flux unit (f.u.) is defined as 10^{-26} Wm^{-2} Hz^{-1} and all coordinates are for epoch 1950·0.

Downloaded from https://academic.oup.com/mnras/article-abstract/160/1/1/2604637 by California Institute of Technology user on 19 May 2020

© Royal Astronomical Society • Provided by the NASA Astrophysics Data System

1972MNRAS.160....1W

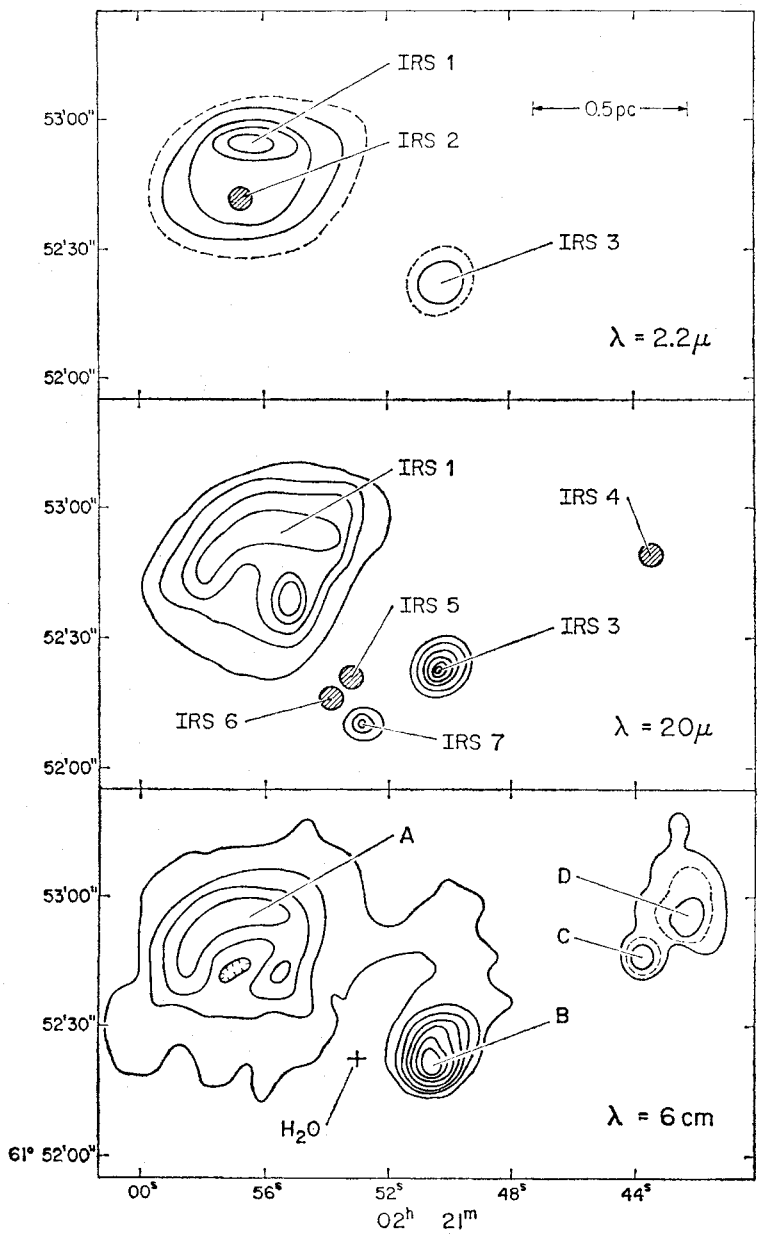

FIG. 1. *The W3 (continuum) region at 2·2-μ, 20-μ and 6-cm wavelength. The complete region was mapped with a 10 arc sec aperture at 2·2 and 20 μ to flux levels of 0·1 and 150 f.u.; the positions and sizes (Table II) of IRS3, IRS4, IRS5, IRS6 and IRS7 were determined with a 5 arc sec aperture. The radio continuum data are taken from Paper I and have a resolution of 6·5 × 7·4 arc sec; the position of the H_2O maser source is as given by Hills* et al. (1972). *The contour intervals, in units of W m^{-2} Hz^{-1} sr^{-1}, are 2·0 × 10^{-19} at 2·2 μ, 2·5 × 10^{-16} at 20 μ and 3·4 × 10^{-18} at 6 cm (T_B = 440 K at 6 cm) with dashed contours at half intervals. Hatched circles indicate unresolved sources. Sources to the west of 02^h 21^m 48^s are not shown at 2·2 μ because of the presence of confusing field stars.*

(a) *IRS1 and IRS2: sources associated with W3(A)*

The bottom two maps of Fig. 1 indicate that the shape and size of IRS1 at 20 μ are nearly identical with those of W3(A) at 6 cm; at both wavelengths emission is concentrated in an incomplete ring surrounding a central region of lower brightness. At 2·2 μ, however, there is an additional unresolved source, IRS2, near the

© Royal Astronomical Society • Provided by the NASA Astrophysics Data System

Downloaded from https://academic.oup.com/mnras/article-abstract/160/1/1/2604637 by California Institute of Technology user on 19 May 2020

1972MNRAS.160....1W

radio minimum. Scans show that its diameter is $\lesssim 5$ arc sec; IRS2 is also observable at 1·65 μ, but was not seen on the 10- and 20-μ scans (flux $\lesssim 100$ f.u. at 20 μ). With the exception of this unresolved source, which for reasons given in Section 4(b) we believe to be an early-type star, there is good agreement between the brightness distributions of W3(A)/IRS1 at 2·2 μ, 20 μ and 6 cm.

The combined radio and infra-red energy distributions of W3(A)/IRS1 are shown in Fig. 2; the flux of IRS2, which is approximately 6 per cent of the total

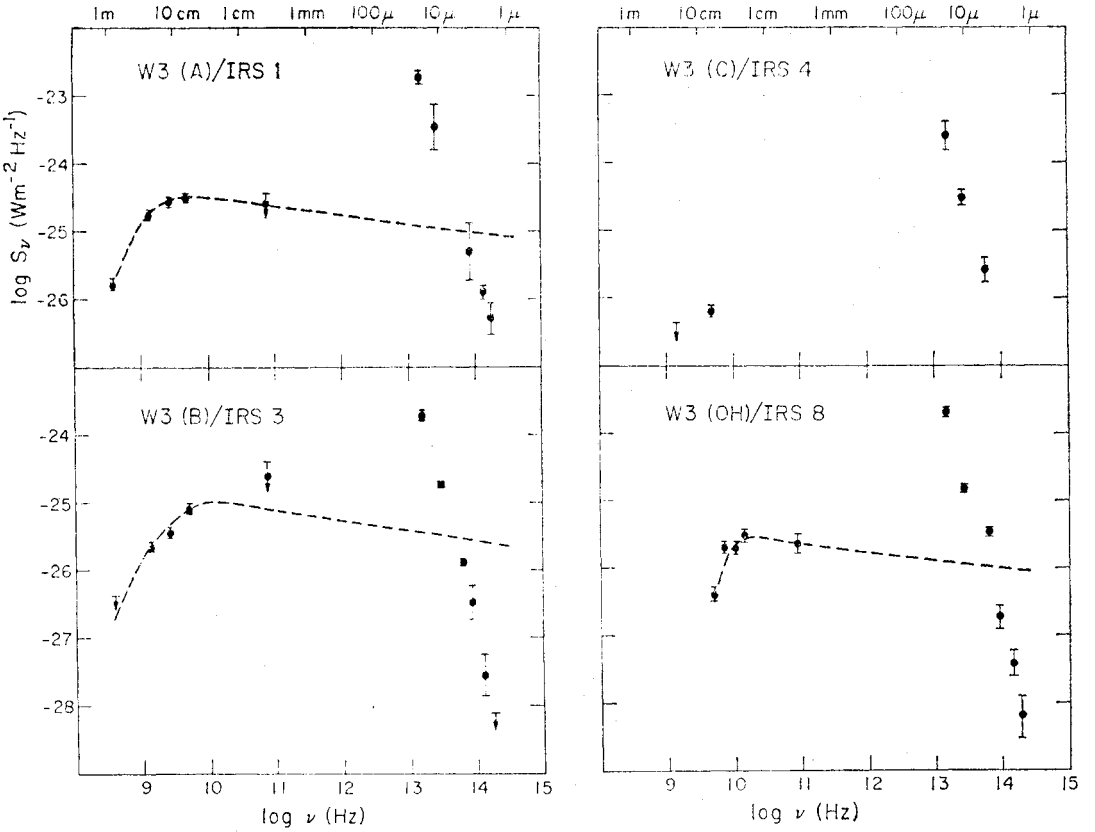

FIG. 2. *The energy distributions of the four sources W3(A)/IRS1, W3(B)/IRS3, W3(C)/IRS4 and W3(OH)/IRS8 at radio and infra-red wavelengths. The dashed lines indicate the expected infra-red thermal emission from the ionized hydrogen as predicted from the radio emission (see Section 4(a)). Radio data are from Paper I (0·4, 1·4 and 5 GHz), Webster & Altenhoff (1970) (2·7 GHz), Aikman (1968), (6·6 and 10·6 GHz), Schraml & Mezger (1969), (15·4 GHz). The 86 GHz point for W3(OH) was supplied by W. J. Wilson (private communication); the 82 GHz limits for W3(A) and W3(B) are from Hobbs, Modali & Maran (1971) who give a value for the total emission for W3 (continuum).*

at 2·2 μ, has not been included. The total flux density at 20 μ was obtained by integration of Fig. 1, but at 2·2 μ, where the source is weaker and the zero level determination more difficult, the total flux density was obtained from a separate series of scans using a 15 arc sec aperture and a signal-reference beam separation of 250 arc sec. The flux densities at 1·65, 3·5, and 10 μ were estimated by normalization of comparative measurements of a 10 to 20 arc sec diameter region of the bright north rim of the source.

The 1- to 3-μ colour of IRS2 is significantly different from that of IRS1; in Table I the 1·65- and 2·2-μ flux densities from IRS2 are compared with those

Downloaded from https://academic.oup.com/mnras/article-abstract/160/1/1/2604637 by California Institute of Technology user on 19 May 2020

© Royal Astronomical Society • Provided by the NASA Astrophysics Data System

1972MNRAS.160....1W

TABLE I

Positions and 2-μ colours of the unresolved source IRS2, and of a 10 arc sec diameter region of the extended source IRS1

	Extended source (IRS1)	Unresolved source (IRS2)
Right ascension (1950·0)	$02^h\,21^m\,56{\cdot}7 \pm 0{\cdot}3^s$	$02^h\,21^m\,56{\cdot}8 \pm 0{\cdot}3^s$
Declination (1950·0)	$61^\circ\,52'\,54 \pm 2''$	$61^\circ\,52'\,42 \pm 2''$
1·65-μ flux density (f.u.)	$0{\cdot}06 \pm 0{\cdot}01$	$0{\cdot}10 \pm 0{\cdot}01$
2·2-μ flux density (f.u.)	$0{\cdot}13 \pm 0{\cdot}01$	$0{\cdot}17 \pm 0{\cdot}01$
Measured ratio ($S_{2\cdot2}/S_{1\cdot65}$)	$2{\cdot}2 \pm 0{\cdot}4$	$1{\cdot}7 \pm 0{\cdot}2$
Predicted ratio ($S_{2\cdot2}/S_{1\cdot65}$) for no extinction	1·15	0·63

from a 10 arc sec diameter region centred on the bright rim of IRS1. The origin of this colour difference is discussed in Sections 4(a) and 4(b).

(b) *IRS3 and IRS4: sources associated with H II condensations*

As can be seen from Fig. 1 and Table II the positions of sources IRS3 and IRS4 agree within experimental error with those of the radio sources W3(B) and W3(C), although there is some indication that IRS4 is displaced from W3(C) in the direction of W3(D). It was possible to measure IRS3 at 3·5 and 2·2 μ (Fig. 2) but the confusion from field stars hindered observations at these wavelengths of IRS4. Scans with a 5 arc sec diameter aperture showed that IRS3 is clearly extended at 20 μ with a size similar to that of W3(B), while IRS4, like W3(C), has a diameter of less than 5 arc sec (see Table II).

TABLE II

Positions, sizes and 20-μ flux densities of infra-red and radio sources

Components	R.A. (1950·0)	Dec. (1950·0)	Approximate size (arc sec)	20-μ flux density (f.u.)
IRS1	$02^h\,21^m\,56{\cdot}0 \pm 0{\cdot}5$	$+61^\circ\,52'\,45 \pm 5''$	40	2000
W3(A)	$02^h\,21^m\,56{\cdot}8 \pm 0{\cdot}4$	$61^\circ\,52'\,49 \pm 5''$	40	—
IRS3	$02^h\,21^m\,50{\cdot}3 \pm 0{\cdot}3^s$	$61^\circ\,52'\,22 \pm 2''$	14	200
W3(B)	$02^h\,21^m\,50{\cdot}7 \pm 0{\cdot}2^s$	$61^\circ\,52'\,21 \pm 2''$	17	—
IRS4	$02^h\,21^m\,43{\cdot}5 \pm 0{\cdot}3^s$	$61^\circ\,52'\,49 \pm 2''$	< 5	300
W3(C)	$02^h\,21^m\,43{\cdot}8 \pm 0{\cdot}2^s$	$61^\circ\,52'\,46 \pm 2''$	< 5	—
W3(D)	$02^h\,21^m\,42{\cdot}4 \pm 0{\cdot}2^s$	$61^\circ\,52'\,55 \pm 2''$	18	—
IRS5	$02^h\,21^m\,53{\cdot}2 \pm 0{\cdot}3^s$	$61^\circ\,52'\,21 \pm 2''$	< 3	500
H_2O	$02^h\,21^m\,52{\cdot}9 \pm 0{\cdot}2^s$	$61^\circ\,52'\,22 \pm 2''$	—	—
IRS6	$02^h\,21^m\,53{\cdot}8 \pm 0{\cdot}3^s$	$61^\circ\,52'\,16 \pm 2''$	< 10	50
IRS7	$02^h\,21^m\,52{\cdot}8 \pm 0{\cdot}3^s$	$61^\circ\,52'\,10 \pm 2''$	5–10	70

The H_2O position is from Hills *et al.* (1972), other radio data from Paper I.

A careful search was made at 20 μ for emission from W3(D), the last of the four radio condensations associated with the W3 (continuum) radio source. Marginal evidence for emission was found on some scans, but it would be safer to conclude only that the 20-μ flux density through a 10 arc sec diameter aperture centred on W3(D) is less than 100 f.u.

Downloaded from https://academic.oup.com/mnras/article-abstract/160/1/1/2604637 by California Institute of Technology user on 19 May 2020

© Royal Astronomical Society • Provided by the NASA Astrophysics Data System

1972MNRAS.160....1W

(c) *IRS5, IRS6 and IRS7: sources not associated with H II condensations*

In addition to the sources associated with H II condensations, three new sources have been discovered at 20 μ which do not correspond to any optical or radio continuum feature. Their locations are shown in Fig. 1 and Table II.

IRS5 is the most remarkable of these sources. Its 20-μ flux density is greater than that of W3(B)/IRS3, despite the fact that it is unresolved with a diameter of less than 3 arc sec (0·05 pc). As can be seen in Fig. 3 its energy distribution is unlike those of the sources associated with H II condensations (Fig. 2), of which IRS3 is typical. It has an extremely steep slope at short wavelengths; between 2·2 and 4·8 μ the flux density increases by a factor of 10^4.

IRS6 and IRS7 are much fainter and were detected only at 20 μ, at which wavelength their flux densities are each about 60 f.u. Measurements on both these sources were difficult owing to their proximity to IRS5, but scans show that IRS7 is extended.

As can be seen in Table II, IRS5 coincides within experimental error with the position of the H_2O maser source as determined by Hills *et al.* (1972). No accurate position is known for the OH emission discovered by Turner (1970) from this region.

(d) *IRS8 and IRS9: sources associated with W3(OH)*

Searches were made at both 2·2 and 20 μ over an area of about 2 arc min diameter centred on W3(OH). The detection limit for the discovery of new sources in this region was 0·07 f.u. at 2·2 μ and 100 f.u. at 20 μ.

Two sources were found; their positions are shown in Table III and their energy distributions in Figs 2 and 4. IRS8 is the more powerful of the two at 20 μ, but IRS9 is the brighter at 2·2 μ.

TABLE III

The two infra-red sources associated with the W3(OH) source

	R.A. (1950·0)	Dec. (1950·0)	Approximate size (arc sec)	20-μ flux density (f.u.)
IRS8	$02^h\ 23^m\ 16{\cdot}7 \pm 0{\cdot}3^s$	$+61°\ 38'\ 56 \pm 2''$	<3	200
Radio continuum	$02^h\ 23^m\ 16{\cdot}48 \pm 0{\cdot}07^s$	$61°\ 38'\ 56{\cdot}8 \pm 0{\cdot}5''$	1·7	—
OH	$02^h\ 23^m\ 16{\cdot}8 \pm 0{\cdot}2^s$	$61°\ 38'\ 54 \pm 2''$	1·2 × 2·3	—
H_2O	$02^h\ 23^m\ 17{\cdot}25 \pm 0{\cdot}2^s$	$61°\ 38'\ 57{\cdot}4 \pm 2''$	—	—
IRS9	$02^h\ 23^m\ 21{\cdot}4 \pm 0{\cdot}3^s$	$61°\ 39'\ 10 \pm 2''$	<10	25

The radio position is from Paper I, the OH position is from Raimond & Eliasson (1969), the OH size from Moran *et al.* (1968), and the H_2O position is from Hills *et al.* (1972).

IRS8 is coincident with the OH and radio continuum positions to within experimental error, though marginally displaced from the H_2O position. It is unresolved at 20 μ, with a diameter less than 3 arc sec. Its energy distribution and luminosity are similar to those of IRS3 and IRS4; at wavelengths less than 3 μ, however, it is difficult to measure because it is superimposed on a fluctuating background.

A preliminary description of IRS9 at 1·65 and 2·2 μ has already been given by Neugebauer, Hilgeman & Becklin (1969); IRS9 is some 30 arc sec away from the

Downloaded from https://academic.oup.com/mnras/article-abstract/160/1/1/2604637 by California Institute of Technology user on 19 May 2020

© Royal Astronomical Society • Provided by the NASA Astrophysics Data System

1972MNRAS.160....1W

OH source and is not associated with any known optical or radio feature. Most of its flux density comes from within a 10 arc sec region, but an accurate estimate of its diameter is difficult owing to the background fluctuations at 2·2 μ mentioned above.

4. DISCUSSION

(a) *Extinction in front of the H II condensations*

The dashed lines in Fig. 2 represent the predicted emission from ionized hydrogen and helium as extrapolated from the radio data using relations given by Willner, Becklin & Visvanathan (1972). This predicted emission includes contributions from free–free, free–bound and bound–bound transitions, but will be referred to simply as ' free–free ' emission for the remainder of this paper.

In the three cases where the radio data are sufficient to permit extrapolation into the infra-red, the measured 2·2- and 1·65-μ emission is well below the predicted ' free–free ' emission. We attribute this deficit to interstellar and circumnebular extinction and estimate the extinction in front of each condensation by comparison of its predicted ' free–free ' and measured 2·2-μ flux density. For W3(A)/IRS1, W3(B)/IRS3 and W3(OH)/IRS8 the ratios of predicted to measured flux density are 5 ± 2, 100 ± 30 and > 25 corresponding to 2·2-μ optical depths of $1{\cdot}6 \pm 0{\cdot}4$, $4{\cdot}6 \pm 0{\cdot}3$ and $> 3{\cdot}2$. These optical depths will be increased if there is significant emission from heated dust at 2 μ.

For IRS1 and IRS2 it is possible to compare the predicted and measured ratios of flux densities at 2·2 and 1·65 μ and thus to derive a value for the extinction in front of the nebula which is essentially independent of radio measurements. The measured and predicted values for this ratio are given in Table I. The predicted ratio for IRS1 is calculated on the basis of ' free–free ' emission (Willner *et al.* 1972); that for IRS2 on the basis that it is an early-type star (Section 4(b)). It is seen from Table I that the measured ratios of $S_{2\cdot2}/S_{1\cdot65}$ are larger by factors of 1·9 and 2·7 for IRS1 and IRS2 over those expected with no extinction. If the obscuring dust obeys a normal interstellar reddening law, the extinction coefficient at 1·65 μ is 1·7 times that at 2·2 μ (Becklin & Neugebauer 1968). Thus the optical depths at 2·2 μ for IRS1 and IRS2 are found to be 0·9 and 1·4, with an error of $\pm 0{\cdot}3$.

There is thus agreement within experimental error for the extinction in front of W3(A)/IRS1 as derived from (a) the ratio of radio to infra-red flux from W3(A)/IRS1; (b) the infra-red reddening of IRS1; and (c) the infra-red reddening of the star IRS2. The fact that the three values for the extinction in front of W3(A)/IRS1 agree within experimental error is justification of the assumptions that (a) IRS2 is a star, and (b) that there is no significant flux from W3(A)/IRS1 at 2·2 μ from processes other than ' free–free ' emission. This latter conclusion is similar to the conclusion of Hilgeman (1970), based on a study of the Brackett-γ emission line, that in the Orion Nebula the thermal emission from dust is less than that from ' free–free ' transitions at 2·2 μ.

The relation between infra-red and optical extinction has been discussed by Becklin & Neugebauer (1968); from their tabulation, the mean 2·2-μ optical depth in front of W3(A)/IRS1 of $1{\cdot}3 \pm 0{\cdot}3$ corresponds to a visual extinction of 14 ± 3 mag. In Paper I a comparison of the radio and Hα brightness of W3 led to the conclusion that the visual obscuration in front of W3(B) is $\geq 14{\cdot}7$ mag. The

Downloaded from https://academic.oup.com/mnras/article-abstract/160/1/1/2604637 by California Institute of Technology user on 19 May 2020

© Royal Astronomical Society • Provided by the NASA Astrophysics Data System

1972MNRAS.160....1W

same argument can be applied to show that the visual extinction in front of W3(A) is $\geq 14{\cdot}0$ mag, in agreement with the value derived from the present infra-red data.

It should be noted that the extinction in front of the condensations varies from source to source, but is apparently uniform in front of the most extended one, W3(A)/IRS1. This suggests that each condensation is associated with its own obscuring matter, the location of which is discussed further in Section 4(c).

(b) *The identification of IRS2 as the exciting star of W3(A)/IRS1*

The possibility that IRS2 is the source of ionizing radiation for the compact H II region W3(A)/IRS1 suggests itself immediately because of (a) the small diameter of the source; (b) its location close to the geometric centre of W3(A); and (c) the fact that its infra-red energy distribution is significantly bluer than that of W3(A)/IRS1.

If IRS2 is at the distance of W3, and its extinction is as discussed in Section 4(a), its absolute magnitude at $2{\cdot}2\ \mu$ is $-5{\cdot}0$. This absolute magnitude corresponds to either an O5 main-sequence or an M3 giant star (Johnson 1966). The ionization attributable to an M3 star would be negligible, but the excitation parameter of an O5 star, a measure of its ionizing flux, is about 100 pc cm^{-2} (Prentice & ter Haar 1969), in agreement with that required, on the basis of radio data (Paper I), to ionize W3(A). Furthermore, the source of ionization is more likely to consist of only one or two very early stars than a larger number of later-type OB stars, because the stellar radiation from such a cluster would have a lower effective temperature and consequently a smaller ultra-violet to infra-red flux ratio than is deduced from the observations.

Finally it should be noted that the apparent visual magnitude for IRS2, if an O5 star hidden behind 14 mag of extinction, would be 20 ± 3 mag, which is compatible with its absence from the Sky Survey prints.

(c) *Dust and infra-red emission from the H II condensations*

While ' free–free ' transitions account satisfactorily for emission shortward of $2{\cdot}2\ \mu$ for W3(A)/IRS1 and, presumably, for the other sources shown in Fig. 2, another emission mechanism must be invoked to explain the large amount of infra-red energy observed in the range 3–20 μ. A widely discussed emission mechanism invoked to explain infra-red emission from galactic sources is that of radiation from heated dust. This proposal is especially attractive since it has been established (Section 4(a)) that obscuring matter exists in the immediate vicinity of the sources.

If the 3- to 20-μ energy originates from hot dust, the dust is probably mixed with the ionizing gas as in M17 (Kleinmann 1970) and the Orion Nebula (Ney & Allen 1969); in this way the marked agreement between the brightness distributions at 20 μ and 6 cm of both W3(A)/IRS1 and W3(B)/IRS3 can be most easily understood. There is no evidence that the infra-red radiation is being emitted from a shell outside the H II region, although, as discussed at the end of this section, most of the obscuring matter must be external to the H II region.

The temperature and optical depth of the emitting dust may be estimated from measured flux densities of those sources which are extended. In Table VI the brightness and colour temperatures based on the 20- and 10-μ fluxes and on two possible emissivity laws are given for IRS3, IRS4, IRS8 and the north rim of

Downloaded from https://academic.oup.com/mnras/article-abstract/160/1/1/2604637 by California Institute of Technology user on 19 May 2020

© Royal Astronomical Society • Provided by the NASA Astrophysics Data System

1972MNRAS.160....1W

TABLE IV

Temperature and optical depths for the dust in the infra-red sources associated with H II condensations

	IRS1	IRS3	IRS4	IRS8
Brightness temperature (K) at 20 μ	65	70	≥ 80	≥ 85
Brightness temperature (K) at 10 μ	95	100	≥ 105	≥ 110
Colour temperature (K) at 20–10 μ for $n = 0$	170	150	160	150
Colour temperature (K) at 20–10 μ for $n = 2$	120	100	110	100
Optical depth at 20 μ for $n = 0$	0·0005	0·004	$\geq 0{\cdot}01$	$\geq 0{\cdot}02$
Optical depth at 20 μ for $n = 2$	0·005	0·03	$\geq 0{\cdot}1$	$\geq 0{\cdot}2$

The emissivity of the dust in the range 10–20 μ is assumed to follow a law $\epsilon \propto \lambda^{-n}$.

IRS1; a diameter of ≤ 5 arc sec was assumed for IRS4 and ≤ 3 arc sec for IRS8. None of the energy distributions can be closely fitted to a blackbody distribution. The temperatures and optical depths probably vary considerably over each source. It may be concluded, however, that: (a) the temperatures of those grains seen at 10 and 20 μ are in the range of 100–200 K; (b) the sources are optically thin at 20 μ; and (c) the more compact sources W3(C)/IRS4 and W3(OH)/IRS8 have significantly larger optical depths at 20 μ than the broader sources W3(A)/IRS1 and W3(B)/IRS3.

Estimates of the particle size and total mass of the dust may be gained from an examination of the radiation equilibrium of the dust in W3(A)/IRS1. If, as was shown in Section 4(b), IRS2 is an O5 star, its luminosity is about $3 \times 10^5 L_\odot$ (Morton & Adams 1968). From Fig. 1 it can be seen that most of the dust is situated at a projected distance of about 0·3 pc from IRS2. A blackbody in thermal equilibrium at this distance from such a star would have a temperature of 25 K. The fact that the grain temperature is almost an order of magnitude higher than this indicates that the emissivity at 20 μ is 10^{-3} less than in the ultra-violet. The most likely explanation for this is that a significant number of the grains have a diameter considerably less than 20 μ. The data are insufficient to allow a determination of how, in detail, the emissivity of the grains varies with wavelength, especially as there are almost certainly real dust temperature variations in the nebula as well as contributions from both ionized hydrogen and exciting stars at shorter wavelengths.

From the optical depths at 20 μ (Table IV) and the ratio of ultra-violet to infra-red emissivity derived above, it may be deduced that the ultra-violet optical depth of the hot dust in the larger condensations W3(A)/IRS1 and W3(B)/IRS3 is of the order unity; the optical extinction due to dust inside the H II region is therefore of the order of 1 mag. This amount of extinction would be caused by 0·1 $M_\odot$ dust at the radius of W3(A)/IRS1, assuming an extinction of 4×10^4 mag g^{-1} cm^2 (Allen 1964). From the radio measurements in Paper I it was concluded that W3(A) contained 14 $M_\odot$ of hydrogen, which leads to a gas to dust ratio on the order of 100, a value which is typical of the interstellar medium. Thus a self-consistent picture for the infra-red emission from the H II condensations may be easily formed on the basis of thermal radiation from dust associated with the ionized gas; it is unnecessary to introduce any special assumptions about the nature or the concentration of the dust.

Downloaded from https://academic.oup.com/mnras/article-abstract/160/1/1/2604637 by California Institute of Technology user on 19 May 2020

© Royal Astronomical Society • Provided by the NASA Astrophysics Data System

1972MNRAS.160....1W

Powerful 100-μ emission at a level of about 10^{-21} W m^{-2} Hz^{-1} has been discovered from H II regions like W3 by Harper & Low (1971) and Hoffmann, Frederick & Emery (1971). The angular resolution available to these observers was comparatively low, but it nevertheless seems probable that much of the 100-μ radiation is emanating from compact regions similar to those described in this paper. In this context it is relevant that the total flux emitted from W3(A)/IRS1 at wavelengths shortward of 20 μ is $10^5\ L_\odot$, which is about one-third of the total available power from IRS2, the star at its centre.

Finally, it may be noted that since the dust mixed with the ionized gas in the H II region contributes only about 1 mag to the visual extinction, W3(A)/IRS1 must be surrounded by a much thicker layer of obscuring dust, with $A_V \approx 13$ mag. This dust is presumably associated with the neutral gas into which the H II region is expanding, but its extent cannot be deduced from the present observations.

(d) *The infra-red source IRS5*

Among the new sources discussed in this paper IRS5 is of particular interest in that (a) it has a very high surface brightness at long wavelengths; (b) it is coincident with an H_2O maser source but no radio continuum source; (c) it is very compact, ≤ 3 arc sec (0·05 pc); and (d) its spectrum is unlike that of those sources that are identified with H II condensations.

The total luminosity of IRS5 for wavelengths shortward of 24 μ is $3 \times 10^4\ L_\odot$. Its energy distribution (Fig. 3) suggests that its temperature is higher than those of

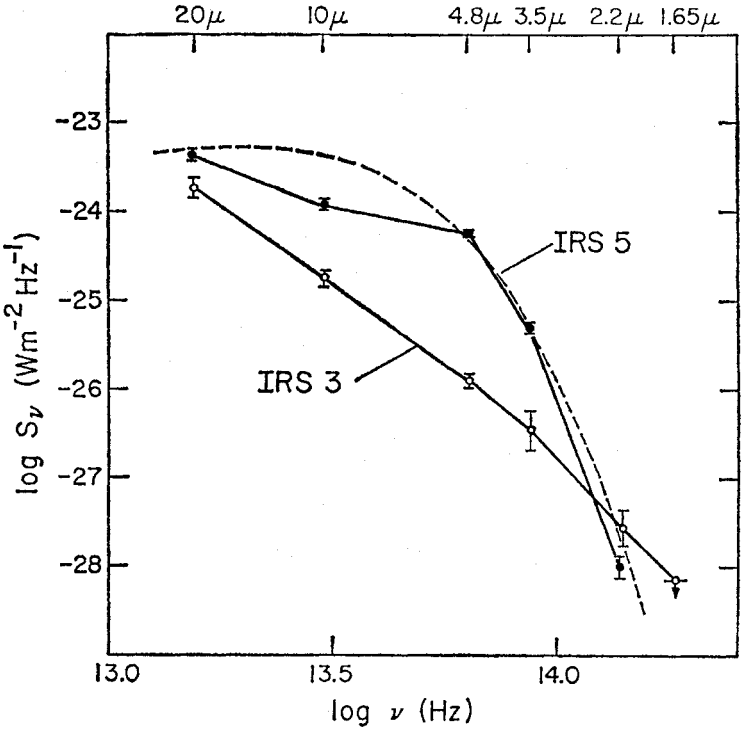

FIG. 3. *The infra-red energy distributions of IRS5 and W3(B)/IRS3. The dashed line is a blackbody curve at a temperature of* 350 *K.*

the H II condensations; if an emissivity of unity and a temperature of 350 K (Fig. 3) is assumed, a diameter of 0·2 arc sec (0·003 pc) is obtained.

© Royal Astronomical Society • Provided by the NASA Astrophysics Data System

Downloaded from https://academic.oup.com/mnras/article-abstract/160/1/1/2604637 by California Institute of Technology user on 19 May 2020

1972MNRAS.160....1W

The nature of the object is very uncertain. Its high luminosity suggests that it could be a dust-enshrouded evolved supergiant or a main-sequence OB star. If it were the latter its excitation parameter would be greater than 30 pc cm^{-2} and it would therefore emit sufficient ultra-violet photons to produce a radio-detectable H II region unless either (a) there is no gas surrounding the star, or (b) the H II region has not expanded sufficiently to make it observable at 5 GHz. The time scale for expansion would be of the order of 10^3 yr, assuming that the ionization front of the nebula moves at 10 km s^{-1}. The unlikely possibility that W3, which is a very young H II region, contains an evolved supergiant star is interesting because such stars, for example VY CMa, are sometimes H_2O emitters like IRS5.

An alternative and exciting possibility for IRS5 is that it is a pre-main-sequence object and that the source of its energy is gravitational rather than thermonuclear.

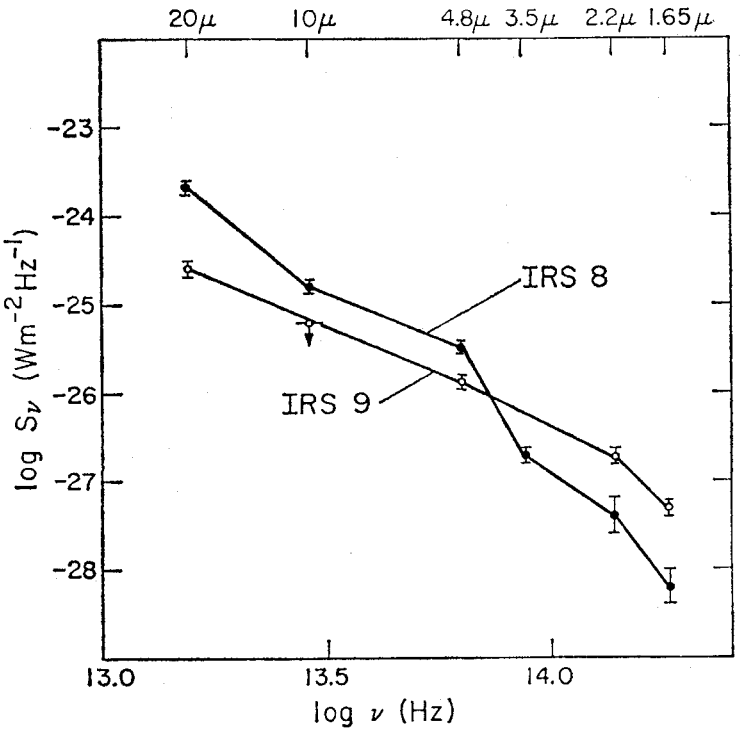

FIG. 4. *The infra-red energy distributions of W3(OH)/IRS8 and IRS9.*

This hypothesis is attractive because of the small diameter of the object, its low temperature and lack of an H II region, its high density as indicated by the presence of molecular maser emission, and its location close to young O stars. Comparison with Larson's (1969) predictions of the infra-red properties of protostars indicates that if IRS5 is a protostar it must have a mass well in excess of 5 $M_\odot$. It is thus possible that IRS5 will subsequently evolve so as to resemble objects like W3(B)/IRS3 or W3(A)/IRS1 when its surface temperature becomes high enough to ionize the surrounding gas. It is perhaps relevant that the intrinsic 20-μ flux from IRS5 is similar to that of the extended infra-red source found by Kleinmann & Low (1967) in the Orion nebula, which Hartmann (1967) has interpreted as being a protostellar cluster. Both sources are unusual in being unassociated with any radio or optical feature except a microwave maser source, but IRS5 is hotter and more compact than the Kleinmann–Low object.

Downloaded from https://academic.oup.com/mnras/article-abstract/160/1/1/2604637 by California Institute of Technology user on 19 May 2020

© Royal Astronomical Society • Provided by the NASA Astrophysics Data System

1972MNRAS.160....1W

Much of the above discussion also applies to the three other sources, IRS6, IRS7 and IRS9, that are unassociated with H II condensations, although IRS6 and IRS7 are so much weaker than W3(B)/IRS3 that the lack of a feature at 6 cm is not significant.

(e) *OH/H_2O maser sources*

Infra-red sources have been discovered within 4 arc sec of both the microwave maser emission regions in W3. In both cases the sources are unresolved and have a high surface brightness at 20 μ. One of these, IRS5, has no associated radio continuum source, while the other, IRS8, is coincident with the W3(OH) continuum radio source, although the latter is faint and is self-absorbed even at 5 GHz. In the wavelength range 3 to 20 μ, IRS5 and IRS8 have an interesting similarity in their energy distribution, in that both seem to have either a deficit at 10 μ or an excess at 5 μ over a smooth distribution; the differences in their energy distribution shortward of 3 μ can be attributed to the presence of 'free–free' emission in W3(OH)/IRS8. Moderate-resolution infra-red spectra of these sources would clearly be of value.

It is profitable to explore the possibility that the OH/H_2O sources are pumped by infra-red transitions as has been discussed by Litvak (1969). For this mechanism the photon flux at the pumping frequency must be greater than the photon flux in the amplified line. The fluxes are calculated in Table V, assuming isotropic

TABLE V

Photon emission rates

Wavelength	Emission rate (10^{45} s^{-1})	
	IRS5	IRS8/W3(OH)
18 cm (OH line)	—	1
1·35 cm (H_2O line)	14	70
20 μ	1·6	0·7
4·8 μ	0·2	0·01

OH data are taken from Robinson & McGee (1967), H_2O from Buhl *et al.* (1969).

emission and a fractional line width of 2×10^{-6}. It can be seen that infra-red pumping of H_2O can be ruled out unless the flux density of W3(OH)/IRS8 increases by at least two more powers of ten longward of 20 μ or either strong infra-red self-absorption or anisotropic emission is postulated. Similarly, infra-red pumping of OH is also unlikely. Thus, despite the very close positional correspondence between maser and infra-red sources, the causal relationship between them is still unclear.

5. CONCLUSIONS

Observations of W3 in the wavelength range 1·65 to 20 μ with spatial resolutions between 5 and 15 arc sec have enabled us to draw the following conclusions:

(1) Four of the five H II condensations discovered at radio continuum wavelengths have associated infra-red sources; the fifth is uncertain. The 3 to 20-μ infra-red emission from these sources is very strong and is attributed

© Royal Astronomical Society • Provided by the NASA Astrophysics Data System

Downloaded from https://academic.oup.com/mnras/article-abstract/160/1/1/2604637 by California Institute of Technology user on 19 May 2020

1972MNRAS.160....1W

to heated dust at temperatures in the range 100–200 K. This dust is closely associated with the ionized hydrogen.

(2) Four infra-red sources have been found which are unassociated with H II condensations. One of these has a luminosity of at least $3 \times 10^4 L_\odot$, a diameter less than 3 arc sec, and may be a massive protostar.

(3) Strong infra-red sources coincide with the OH and H_2O maser sources. Simple infra-red pumping models do not work in the case of H_2O, and are unlikely in the case of OH.

(4) The exciting source of one of the H II condensations has been identified as an unresolved source which is observable around 2 μ and is probably an O5 star.

(5) The presence of large quantities of interstellar or circumnebular extinction is confirmed. The amount of extinction varies, but reaches 50 visual magnitudes in front of W3(B).

ACKNOWLEDGMENTS

This work could not have been done without the support of the Caltech infra-red group; we especially thank J. Bennett, G. Forrester and L. Roberts for their assistance. We further thank T. Hilgeman who made some of the early infra-red measurements of W3 with us, and our night assistants E. Hancock and J. Corresco for their help. Radio data were provided prior to publication by W. J. Wilson, and by R. Hills and W. J. Welch. P. Conti and C. R. O'Dell kindly commented on an early version of this paper. C.G.W-W. is grateful to the Commonwealth Fund for the receipt of a Harkness Fellowship and to Hale Observatories for guest observer's privileges. This work was supported in part by National Aeronautics and Space Administration Grants NGL 05-002-007 and NGL 05-002-207.

C. G. Wynn-Williams:
California Institute of Technology

E. E. Becklin and G. Neugebauer:
Hale Observatories, California Institute of Technology and Carnegie Institution of Washington

REFERENCES

Aikman, G. C., 1968. M.S. Thesis, University of Toronto.
Allen, C. W., 1964. *Astrophysical Quantities*, 2nd edition, p. 252, The Athlone Press, London.
Becker, W., 1963. *Z. Astrophys.*, **57**, 117.
Becklin, E. E. & Neugebauer, G., 1968. *Astrophys. J.*, **151**, 145.
Buhl, D., Snyder, L. E., Schwartz, P. R. & Barrett, A. H., 1969. *Astrophys. J.*, **158**, L97.
Harper, D. A. & Low, F. J., 1971. *Astrophys. J.*, **165**, L9.
Hartmann, W. K., 1967. *Astrophys. J.*, **149**, L87.
Hilgeman, T., 1970. Ph.D. Thesis, California Institute of Technology.
Hills, R., Janssen, M. A., Thornton, D. D. & Welch, W. J., 1972. *Astrophys. J.*, **175**, L59.
Hobbs, R. W., Modali, S. B. & Maran, S. P., 1971. *Astrophys. J.*, **165**, L87.
Hoffmann, W. F., Frederick, C. L. & Emery, R. J., 1971. *Astrophys. J.*, **170**, L89.
Johnson, H. L., 1966. *A. Rev. Astr. Astrophys.*, **4**, 193.
Kleinmann, D. E., 1970. *Bull. Am. astr. Soc.*, **2**, 325.
Kleinmann, D. E. & Low, F. J., 1967. *Astrophys. J.*, **149**, L1.
Larson, R. B., 1969. *Mon. Not. R. astr. Soc.*, **145**, 297.

Downloaded from https://academic.oup.com/mnras/article-abstract/160/1/1/2604637 by California Institute of Technology user on 19 May 2020

© Royal Astronomical Society • Provided by the NASA Astrophysics Data System

1972MNRAS.160....1W

Litvak, M. M., 1969. *Astrophys. J.*, **156**, 471.
Moran, J. M., Burke, B. F., Barrett, A. H., Rogers, A. E. E., Ball, J. A., Carter, J. C. & Cudaback, D. D., 1968. *Astrophys. J.*, **152**, L97.
Morton, D. C. & Adams, T. F., 1968. *Astrophys. J.*, **151**, 611.
Neugebauer, G., Hilgeman, T. & Becklin, E. E., 1969. *Bull. Am. astr. Soc.*, **1**, 201.
Ney, E. P. & Allen, D. A., 1969. *Astrophys. J.*, **155**, L193.
Prentice, A. J. R. & Haar, D. ter, 1969. *Mon. Not. R. astr. Soc.*, **146**, 423.
Raimond, E. & Eliasson, B., 1969. *Astrophys. J.*, **155**, 817.
Reifenstein, E. C. III, Wilson, T. L., Burke, B. F., Mezger, P. G. & Altenhoff, W. J., 1970. *Astr. Astrophys.*, **4**, 357.
Robinson, B. J. & McGee, R. X., 1967. *A. Rev. Astr. Astrophys.*, **5**, 183.
Schild, R., Peterson, D. M. & Oke, J. B., 1971. *Astrophys. J.*, **166**, 95.
Schraml, J. & Mezger, P. G., 1969. *Astrophys. J.*, **156**, 269.
Turner, B. E., 1970. *Astrophys. Lett.*, **6**, 99.
Webster, W. J. & Altenhoff, W. J., 1970. *Astr. J.*, **75**, 896.
Willner, S. P., Becklin, E. E. & Visvanathan, N., 1972. *Astrophys. J.*, **175**, 699.
Wilson, W. J., Schwartz, P. R., Neugebauer, G., Harvey, P. H. & Becklin, E. E., 1972. *Astrophys. J.*, **177**, in press.
Wynn-Williams, C. G., 1971. *Mon. Not. R. astr. Soc.*, **151**, 397.

Downloaded from https://academic.oup.com/mnras/article-abstract/160/1/1/2604637 by California Institute of Technology user on 19 May 2020

© Royal Astronomical Society • Provided by the NASA Astrophysics Data System